NJC

Accepted Manuscript

This is an *Accepted Manuscript*, which has been through the Royal Society of Chemistry peer review process and has been accepted for publication.

Accepted Manuscripts are published online shortly after acceptance, before technical editing, formatting and proof reading. Using this free service, authors can make their results available to the community, in citable form, before we publish the edited article. We will replace this *Accepted Manuscript* with the edited and formatted *Advance Article* as soon as it is available.

You can find more information about *Accepted Manuscripts* in the Information for Authors.

Please note that technical editing may introduce minor changes to the text and/or graphics, which may alter content. The journal's standard Terms & Conditions and the Ethical guidelines still apply. In no event shall the Royal Society of Chemistry be held responsible for any errors or omissions in this *Accepted Manuscript* or any consequences arising from the use of any information it contains.

ROYAL SOCIETY OF CHEMISTRY

www.rsc.org/njc

NJC

RSCPublishing

ARTICLE

Hydrogen-bonded chiral molecular switches: Photo and thermally reversible switchable full range color in self-organized helical superstructure

Cite this: DOI: 10.1039/x0xx00000x

Received ooth January 2012,
Accepted ooth January 2012

DOI: 10.1039/x0xx00000x

www.rsc.org/

Ouyu Jin, Dengwei Fu, Yixiu Ge, Jie Wei, Jinbao Guo*

In this study, a new kind of hydrogen-bonded (H-bonded) chiral molecular switches (CMS) composed of azobenzene moieties as photo-responsive parts and H-bonded complexes as thermo-responsive parts was developed. Photo and thermally reversible switching behavior of cholesteric liquid crystals (Ch-LCs) based on the H-bonded CMS was detailedly investigated. The results demonstrate that H-bonded CMS undergo a trans-cis photoisomerization under UV light, which results in the decrease of helical twisting power (HTP). Meanwhile, the modulation of the intermolecular forces between proton donors and acceptors with temperature has a positive influence on the change of HTP. Reversible blue, green, and red reflections of the self-organized helical superstructure could be achieved under UV/Vis light as well as with temperature change. According to the geometry optimization based on Gaussian 03 calculations at the B3LYP/6-31G(d) level, the molecular aspect ratio could be considered to be one of the important factors influencing the HTP of H-bonded CMS. This dynamic tuning of the self-organized helical superstructure based on dual and selective molecular mechanism opens up a way to achieve a new kind of LCs photonic materials.

Introduction

Cholesteric liquid crystals (Ch-LCs), which are characterized by their self-organized helical superstructure, have attracted tremendous attention because of their unique optical properties such as selective reflectivity.[1] The pitch refers to the distance over which the LC molecules undergo a full 360° twist and the wavelength of maximum reflection can be described as below: $\lambda_{max}=n*P$, where λ_{max} is the spectral position of the reflection, n is the average refractive index and P is the pitch.[2] As shown in the equation, the pitch, which is sensitive to external stimuli, plays a very important role in tuning the selective reflection band (SRB) of Ch-LCs. It is widely acknowledged that when achiral nematic liquid crystals (N-LCs) are doped with chiral compounds, they will be transformed into Ch-LCs.[3] Since the pitch length of Ch-LCs is sensitive to external factors including heat,[4] light irradiation,[5] and force,[6] stimuli-responsive Ch-LCs are expected，which has been a focus of extensive research interest in the past few decades.[7]

Due to the advantages of ease addressability, fast response time and the potential for remote control,[8] a lot of investigations have been carried out on photoinduced optical responses of Ch-LCs.[9] A widely studied class of photoactive molecular switches is photochromic compounds including azobenzenes,[10] dithienylethenes,[11,12] etc. Azobenzene and its derivatives, which are most commonly used dopants, undergo *trans-cis* and *cis-trans* isomerization upon UV/Vis irradiation while *cis* and *trans* isomers of them are bent and rod-like in shape respectively. Studies have proved that conformation difference of azobenzene compound induced by light irradiation contributes a lot to affecting helical twisting power (HTP) of chiral dopants so that we can obtain photoresponsive Ch-LCs based on such molecular switches. Among them, Li *et al.* reported reversible photo-responsive Ch-LCs containing an azobenzene moiety with a short flexible carbonyldioxy spacer and a polar carbonyl unit in a terminal chain and the reversible photoresponsive properties were well demonstrated by UV irradiation. Furthermore, Li *et al*. also reported a light driven nanoscale chiral molecular switch capable of phototuning reflection color across the full visible spectrum due to the photoisomerization of binaphthyl azobenzene groups and the HTP of the molecular switch was 304 μm^{-1} (at initial state) and 89 μm^{-1} (at photostationary state).[13]

Moreover, hydrogen bonding (H-bond), a typical way for assembling molecules and achieving supramolecular structures, has been an attractive way to construct stimuli-responsive materials.[14] For example, owing to the interaction of H-bond donor and acceptor, H-bonded chiral monomers can be used as molecular triggers to obtain Ch-LCs polymer network materials that change the reflection color by a change in temperature as well as the change in pH.[15,16] Recently, optical sensors based on

H-bonded Ch-LCs networks are nicely illustrated by Herzer *et al.*[17] Optical sensors they made can respond to temperature and humidity by changing its reflection color.

In this work, we developed a facile method to obtain dual responsive Ch-LCs by fabricating a new kind of H-bonded chiral molecular switches (CMS), in which binaphthyl azobenzene molecule is used as the proton acceptor, and four chiral and achiral acids are proton donors. Here we note that, the complicated synthesis of CMS was simplified due to the easy H-bonded assembly process. Based on the H-bonded CMS, the photo and thermo responsive behavior of Ch-LCs was investigated in detail. Herein, we focus on the influence of molecular structure of the proton donors on the HTP of H-bonded CMS and the corresponding switching effects. Additionally, we utilize the molecular simulation to estimate the relationship between molecular structure of H-bonded CMS and the HTP, the change in HTP and the switching mechanism. The main practical objective of this work is to develop a relatively simple and effective approach to fabricate a new kind of responsive LCs photonic materials.

Experimental Section

Materials

In this study, SLC1717 (isotropic temperature, Ti=92 °C; 20 °C，589 nm, Δn=0.201, Slichem Liquid Crystal Material Co., Ltd.), (S)-(+)-2-Octanol, (R)-(-)-2-Octanol (Beijing Lyra Material-Tech Co., Ltd.) were used. 4-(Decyloxy)benzoic acid, (DBA) (S)-(+)-2-Methylbutyric acid (MBA) were purchased from Sigma-Aldrich. Isonicotinoylchloride hydrochloride was synthesized as described in our previous paper.[15] The proton acceptor, 4,4'- ((S)-[1,1'-binaphthalene]-2,2'-diyl)bis(diazene-2,1-diyl))diphenol isonicotinate (BNAzo) and the proton donors, (S)-4'-(octan-2-yloxy)-[1,1'-biphenyl]-4-carboxylic acid ((S)-OyBp), (R)-4'-(octan-2-yloxy)-[1,1'-biphenyl]-4-carboxylic acid ((R)-OyBp) were synthesized following the procedures as shown in Scheme 1.

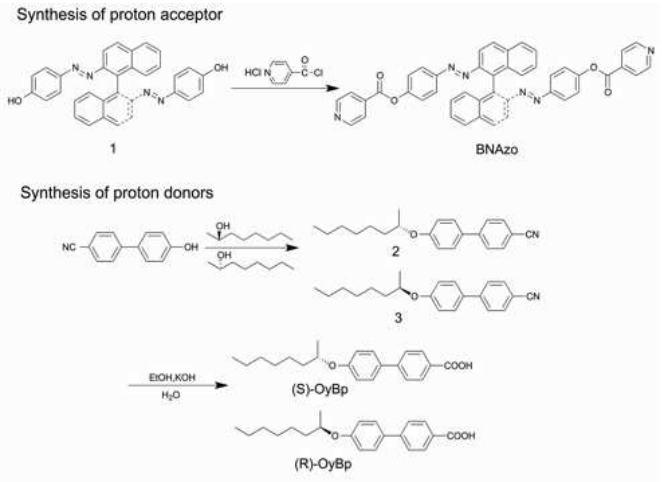

Scheme 1. Synthetic routes to the proton acceptor and donors of H-bonded CMS.

Synthesis of H-bonded proton acceptor

i Compound 1

4,4'-((S)-[1,1'-binaphthalene]-2,2'-diyl)bis(diazene-2,1-diyl))diphenol:

Compound 1 was synthesized according to the procedure written in previous work.[9i,18]

^{1}H NMR (400MHz, DMSO): δ= 10.18 (s, 2H, Ar-OH), 8.18 (d, J=8.9Hz, 2H, Ar-H), 8.10 (m, 4H, Ar-H), 7.57 (t, J=7.5Hz, 2H, Ar-H), 7.35 (t, J=8.1Hz, 2H, Ar-H), 7.28 (d, J=8.35Hz, 2H, Ar-H), 7.18 (d, J=8.73Hz, 4H, Ar-H), 6.70 (d, J=8.73Hz, 4H, Ar-H).

ii BNAzo

((S)-[1,1'-binaphthalene]-2,2'-diyl)bis(diazene-2,1-diyl))diphenol isonicotinate (H-bonded proton acceptor):

To a stirred suspension of isonicotinoyl chloride hydrochloride (0.07 g, 0.4 mmol) in THF (10 ml), triethylamine (0.45 ml) was added slowly. A solution of Compound (0.1 g, 0.2 mmol) dissolved in THF (5 ml) was added dropwise into the above suspension. The mixture was continuously stirred at room temperature for 72 h, filtered and concentrated in vacuum. The precipitate was washed with distilled water several times and then filtered and purified by column chromatography to obtain red solid, Yield, 50%.

^{1}H NMR (400MHz, Acetone): δ= 8.88 (d, J=4.56Hz, 4H, N-H), 8.18 (d,J=9.2Hz, 2H, Ar-H), 8.11 (d, J=7.92Hz, 2H, Ar-H), 8.02 (t, J=4.68Hz, 4H, N-H), 7.57 (t, J=7.4Hz, 2H, Ar-H), 7.50 (d, J=8.36Hz, 2H, Ar-H), 7.42 (d, J=8.8Hz, 4H, Ar-H), 7.35 (m, 4H, Ar-H), 7.14 (d, J=8.76Hz, 4H, Ar-H).

IR (thin film) ν_{max}: 2969, 1744, 1596, 1489, 1408, 1263, 1220, 1061 and 749cm^{-1}.

^{13}C NMR ($CDCl_3$) δ=163.27, 151.88,150.83, 150.49, 148.20, 137.68, 136.85, 134.59, 134.18, 130.91, 129.28, 128.84, 128.17, 127.89, 127.53, 126.89, 124.11, 123.32, 121.76, 114.15, 77.33, 77.01, 76.69, 65.57, 30.58, 19.19, 13.73.

High Resolution MS (M+H) calcd for $C_{44}H_{28}N_6O_4$: 705.2200, found: 705.2249.

Synthesis of H-bonded proton donor

i Compound 2

(S)-4'-(octan-2-yloxy)-[1,1'-biphenyl]-4-carbonitrite:

Under the protection of nitrogen, we dissolved 4'-Hydroxy-4-biphenylcarbonitrile (4.88 g, 25 mmol), (R)-(-)-2-Octanol (3.25 g, 25 mmol) and triphenylphosphine (8.36 g, 27.5 mmol) in dry THF (50 ml), cool to 0 °C using an ice-bath and slowly add the DIAD (7.6 g, 0.0375 mmol) dissolved in THF, then stir at room temperature for 12 hours. After removing bulk solvents, the orange oily mixture was purified by column chromatography to get colorless oil, Yield, 85%.

^{1}H NMR (400MHz, $CDCl_3$): δ=7.70-7.64(m, 4H, Ar-H), 7.55(d, J=8.72Hz, 2H, Ar-H, 7.01(d, J=8.72Hz, 2H, Ar-H),

4.45(m, 1H, -OCH), 1.63(m, 3H, -OCHCH$_3$), 1.36-1.33 (m, 10H, CH$_2$), 0.92(t, J=6.56Hz, 3H, CH$_3$).
IR (thin film) ν_{max}: 2929, 2855, 2225, 1602, 1520, 1492, 1246, 1178 and 821 cm^{-1}.

Compoud 3 was synthesized following similar procedures mentioned above, Yield, 87%.
^{1}H NMR (400MHz, CDCl$_3$): δ=7.70-7.64(m, 4H, Ar-H), 7.54(d, J=9.12Hz, 2H, Ar-H, 7.01(d, J=8.76Hz, 2H, Ar-H), 4.45(m, 1H, -OCH), 1.62(m, 3H, -OCHCH$_3$), 1.36-1.33(m, 10H, CH$_2$), 0.92(t, J=6.92Hz, 3H, CH$_3$).
IR (thin film) ν_{max}: 2929, 2855, 2225, 1602, 1520, 1492, 1246, 1178 and 821 cm^{-1}.

ii **(S)-OyBp**

(S)-4'-(octan-2-yloxy)-[1,1'-biphenyl]-4-carboxylic acid:

Under the protection of nitrogen, (S)-4'-(octan-2-yloxy)-[1,1'-biphenyl]-4- carbonitrite (3.08 g, 10 mmol), 40 ml of water, 40 ml of ethanol and aqueous solution of KOH (0.1g/10ml) were introduced into a stirring apparatus. The mixture was heated under reflux and allowed to react at this temperature for about 10 hours. After being cooled to room temperature, the mixture was neutralized by addition of hydrochloric acid until PH=7. The water was then distilled off in vacuum. The residue was taken up in ethanol and the insoluble salts were filtered off. The solvent of the filtrate was removed in vacuum to get white powder, Yield, 89%.
^{1}H NMR (400MHz, DMSO): δ=12.92(s, 1H, Ar-COOH), 7.94(d, J=8.32Hz, 2H, Ar-H), 7.68(m, 4H, Ar-H), 7.02(m, 2H, Ar-H), 4.50(m, 1H, -OCH), 1.66(m, 3H, -OCHCH$_3$), 1.40-1.25(m, 10H, CH$_2$), 0.86(t, J=6.48Hz, 3H, CH$_3$)
IR (thin film) ν_{max}: 3201, 2928, 2857, 1603, 1524, 1246, 1192, 831 and 776 cm^{-1}.

iii **(R)-OyBp**

(R)-4'-(octan-2-yloxy)-[1,1'-biphenyl]-4-carboxylic acid:

(R)-OyBp was synthesized following similar procedures mentioned above, Yield, 80%.
^{1}H NMR (400MHz, DMSO): δ=12.94(s, 1H, Ar-COOH), 7.94(d, J=8.28Hz, 2H, Ar-H), 7.68(m, 4H, Ar-H), 7.01(m, 2H, Ar-H), 4.50(m, 1H, -OCH), 1.67(m, 3H, -OCHCH$_3$), 1.42-1.25(m, 10H, CH$_2$), 0.86(t, J=6.44Hz, 3H, CH$_3$)
IR (thin film) ν_{max}: 3208, 2928, 2857, 1603, 1523, 1245, 1192, 831 and 776 cm^{-1}.

Preparation of H-bonded chiral molecular switches

H-bonded CMS were obtained by mixing the proton acceptor (BNAzo) with four proton donors (MBA, DBA, (S)-OyBp and (R)-OyBp) in molar ratio of 1:2 in THF respectively, followed by slow evaporation. Figure 1 shows the chemical structures of four proton donors (MBA, DBA, (S)-OyBp and (R)-OyBp) and the corresponding H-bonded CMS (BNAzo-MBA, BNAzo-DBA, BNAzo-(S)-OyBp and BNAzo-(R)-OyBp). Then we doped these H-bonded CMS with N-LCs host (SLC1717) to get Ch-LCs with the light and temperature dual stimuli-responsive behavior, the Ch-LCs molecular arrangements and the corresponding switching mechanisms are demonstrated in Figure 2.

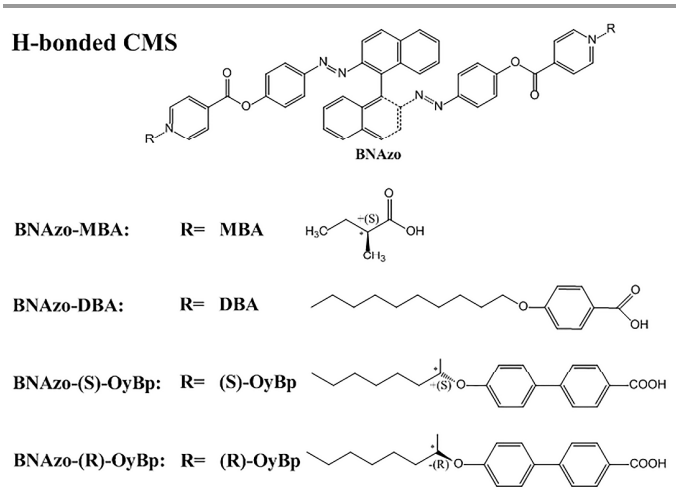

Figure 1. The chemical structures of H-bonded CMS and proton donors we used here

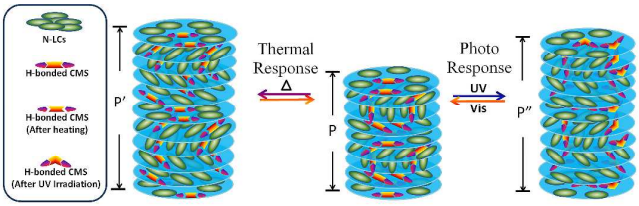

Figure 2. The schematic of the helical superstructure and the corresponding switching mechanism of H-bonded CMS in N-LCs host reversibly dynamically tuned by UV/vis light and heat.

Measurements

The H-bonded CMS were characterized by FT-IR spectroscopy and variable-temperature FT-IR spectroscopy. The FT-IR spectra were recorded on a Nicolet 5700 spectrometer at frequencies ranging from 400-4000 cm^{-1}. The samples were observed by POM (Leica DM2500P) with a hot stage calibrated with an accuracy of ± 0.1 °C (Linkam, THBS-600). The reflection spectra were examined with AvaSpec-2048 spectrophotometer in reflection mode. UV-vis and CD spectrum of H-bonded CMS (in 1,4-dioxane) were taken by a JASCO J810 spectrometer and a JASCO V550 spectrometer, respectively. UV irradiation was carried out by mercury arc lamp (Powerarc UV 100) through a filter at 365 nm.

Results and Discussion

In this study, the H-bonded CMS (BNAzo-MBA, BNAzo-DBA, BNAzo-(S)-OyBp and BNAzo-(R)-OyBp) were obtained by the self-assembly method. The effects of the configuration of chiral centers and introduction of proton donors on HTP of the H-bonded CMS were addressed detailedly. Firstly, we used FT-IR spectrometry to distinguish the existence and intensity of H-bonding in this work. There are two strong H-bond self-

assembly processes in our system, including the –OH…N between proton donors and acceptors and the –OH…O=C- between carboxylic acid dimers. Since the former being relatively stronger than the latter,[19] given the appropriate proportion of donors and acceptors, the chiral pyridine derivative molecules are prone to combine with carboxylic acid molecules instead of the formation of carboxylic acid dimers. Figure 3 shows the FT-IR spectra of the H-bonded CMS and their precursors. The FT-IR spectra confirm the presence of H-bonding obtained by self-assembly process. As shown in Figure 3, two peaks around 2500 and 1900 cm^{-1} indicate the presence of hydrogen bonds, which almost coincides with the position of –OH stretching of H-bond between the carboxylic acid and pyridyl group. Figure 3a shows that the intensity of peaks at 2720 and 2545 cm^{-1} decreased, which means the H-bonds between –OH…N have taken place of the bonds of MBA dimers. Similarly, such phenomenon can also be observed in BNAzo-DBA, BNAzo-(S)-OyBp, BNAzo-(R)-OyBp as shown in Figure 3b, 3c and 3d indicating that four H-bonded CMS molecules with different proton donors were successfully assembled.

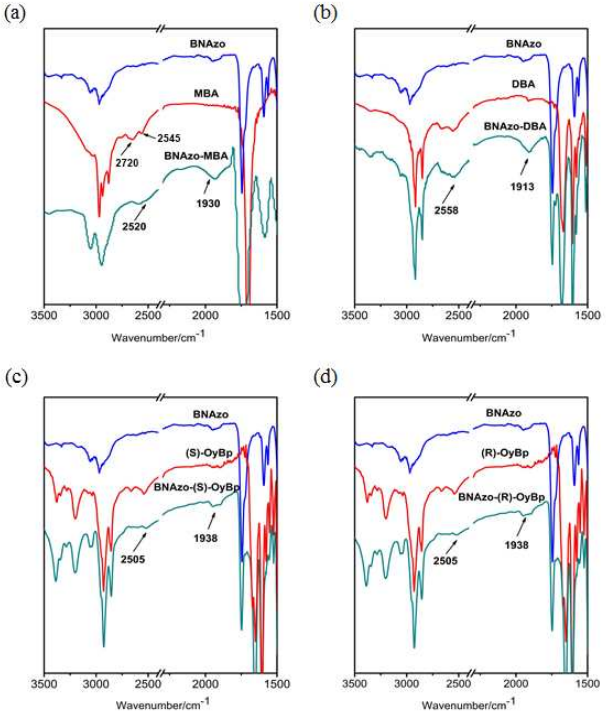

Figure 3. FT-IR spectra of the H-boned CMS and their precursors (a): BNAzo-MBA, BNAzo, MBA; (b): BNAzo-DBA, BNAzo, DBA; (c): BNAzo-(S)-OyBp, BNAzo, (S)-OyBp; (d): BNAzo-(R)-OyBp, BNAzo, (R)-OyBp.

In Figure 4, the thermal stability of the H-bonded CMS was studied by the variable-temperature FT-IR spectroscopy. With the temperature increasing, the peaks indicating the H-bonds between the -OH and pyridyl group (around 2500 and 1900 cm^{-1}) became weaker (as the inset shows), which means the elevation of temperature affected interaction between proton donors and acceptors. We can also find that the four groups of H-bonded CMS (BNAzo-MBA, BNAzo-DBA, BNAzo-(S)-OyBp and BNAzo-(R)-OyBp) have good thermal stability across a temperature range of 30 °C to 110 °C, which sufficiently satisfy our experimental condition.

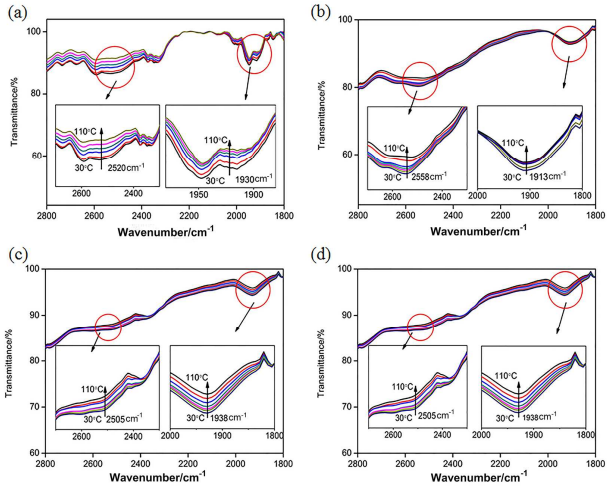

Figure 4. Variable-temperature FT-IR spectra of H-bonded CMS (a): BNAzo-MBA; (b): BNAzo-DBA, (c): BNAzo-(S)-OyBp, (d): BNAzo-(R)-OyBp.

In our study, azobenzene moiety was introduced, which can be a photoresponsive part in H-bonded CMS. The effect of UV irradiation on the four H-bonded CMS (in 1,4-dioxane) was studied by circular dichroism (CD) spectroscopy and UV-vis spectroscopy. Figure 5 and Figure 6 show the change in UV and CD spectra of BNAzo-MBA (a), BNAzo-DBA (b), BNAzo-(S)-OyBp (c) and BNAzo-(R)-OyBp (d) under various UV irradiation condition. Studies shows that the *trans* form of the azobenzene in BNAzo exhibited absorption maxima at 360 nm due to a π-π* transition and at 440 nm due to an n-π* transition.[9f,21] It is found that after photoirradiation at 365 nm (2 $mW \cdot cm^{-2}$), there is a decrease in the π-π* band and a relatively small amount of increase in the n-π* band, which indicates that *trans-cis* photoisomerization of BNAzo takes place on photoirradiation. Meanwhile, as shown in Figure 6, CD spectra exhibit distinct bands for n-π* and π-π* transitions of the azochromophore. For example, at initial state, BNAzo-MBA shows a negative band and positive band for the π-π* transitions at 320 nm and 380 nm respectively followed by a relatively weak negative band at 450 nm, upon UV irradiation (365 nm, 2 $mW \cdot cm^{-2}$), with the influence of photoisomerization of azobenzene moieties, we can find a gradual increase at 450nm due to the formation of cis isomer, and the pattern of CD Cotton effect between 300 and 400 nm become weak due to the π-π* transitions, which is corresponding to the phenomenon we observed in UV-vis spectra. Moreover, to prove the photoisomerization of azobenzene has no impact on the thermoresponsive behavior in this work, we measured the change in absorption of four H-bonded CMS in 1,4-dioxane at various temperatures. UV-vis spectra show nearly no change is found in the absorption spectra, which indicates that photoisomerization of azobenzene structure does not take place

during heat treatment process, therefore, the light and temperature switching processes of H-bonded CMS are two separative processes.

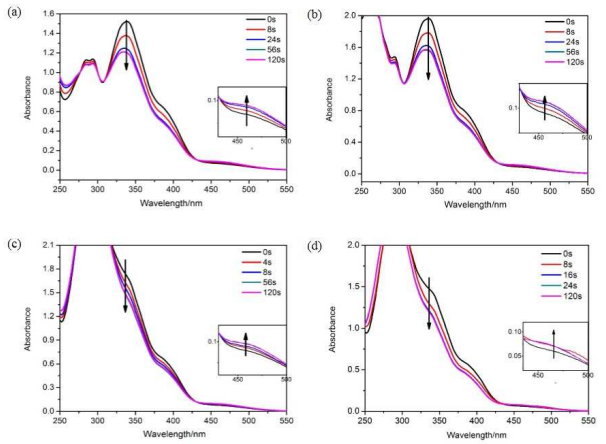

Figure 5. UV-vis absorption spectra of H-bonded CMS in 1,4-dioxane under UV irradiation (a): BNAzo-MBA; (b): BNAzo-DBA, (c): BNAzo-(S)-OyBp, (d): BNAzo-(R)-OyBp.

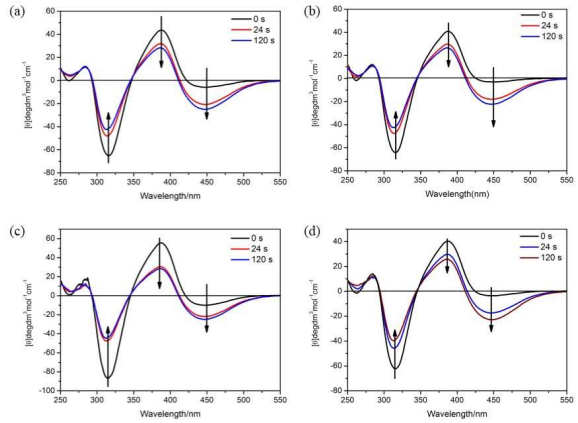

Figure 6. CD spectra of H-bonded CMS in 1,4-dioxane under UV irradiation (a): BNAzo-MBA; (b): BNAzo-DBA, (c): BNAzo-(S)-OyBp, (d): BNAzo-(R)-OyBp.

Furthermore, we studied photo and thermoresponsive behavior of H-bonded CMS in the commercially available N-LCs host (SLC1717) by using the Grandjean-Cano method. The HTP value was used to characterize the ability of chiral dopant for twisting cholesteric mesophase and it is defined as the value of β and expressed by following equation: β=1/Pc, where P is the helical pitch and c is the concentration of the chiral dopant. Four LCs samples were prepared by mixing the H-bonded CMS with SLC1717 in CH_2Cl_2, followed by the removal of solvent, the weight ratios of which are corresponding to chiral dopant (BNAzo-MBA, BNAzo-DBA, BNAzo-(S)-OyBp and BNAzo-(R)-OyBp) : SLC1717 host =1:99 respectively. Moreover, to further discuss how the introduction of proton donors impacts the phototunability of proton acceptor (BNAzo) and to make sure the H-bonds really contribute to the temperature dependence of HTP value of Ch-LCs, we also prepared samples by mixing the BNAzo (1 wt%) with SLC1717. Then we put the mixtures into wedges cell, which had been coated with

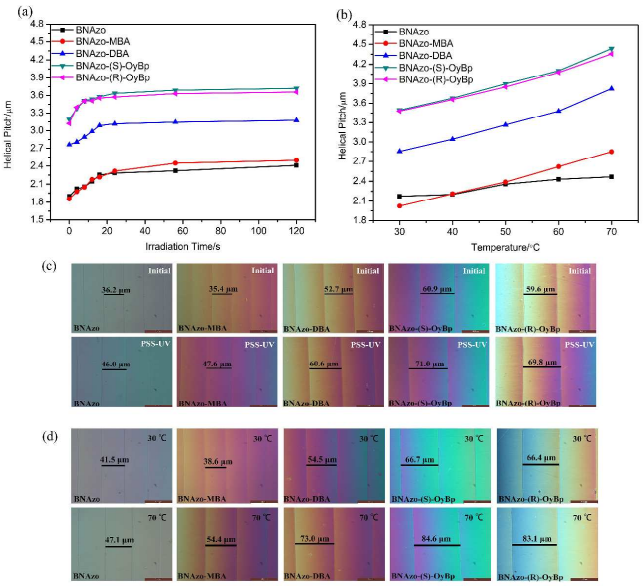

Figure 7. Changes in the helical pitch of 1.0 wt% H-bonded CMS in SLC1717 (a) upon UV irradiation; (b) at various temperatures and POM micrographs of Cano wedge cells (c) upon UV irradiation; (d) at various temperatures.

polyimide and rubbed to align LC moieties. Owing to the twisting ability of H-bonded CMS, the N-LCs host is induced to exhibit helical structure so we can see Cano lines by using POM (Figure 7c and 7d). The phototunability behavior of LC host was observed by measuring the change in distance between Cano lines under UV irradiation. As Figure 7c shows, the distance between Cano lines of BNAzo-(S)-OyBp is 60.9 μm at initial state and it increases to 71 μm after irradiation with UV light, and other four Ch-LCs samples show the same trends during the photoisomerization process. Using the Cano wedge method, the pitch length can be determined according to the equation: p= 2Rtanθ, where R represents the distance between the Cano lines and θ is the wedge angle (θ=1.5°, tanθ=0.0262). The helical pitch length of these H-bonded CMS increase upon UV irradiation from initial state to photostationary state (PSS-UV), which means the HTP values of the H-bonded CMS decrease because of the *trans* to *cis* photoisomerization. For instance, before UV light irradiation at 365 nm, pitch length of BNAzo-MBA is 1.85 μm while after UV irradiation for 120 s, the length of helical pitch increase to 2.49 μm due to photoisomerization process of azobenzene moieties, which is corresponding to the change of distance between Cano lines as discussed above. As mentioned above, upon UV irradiation, photoisomerization of rod shaped *trans* isomer to bent *cis* isomer happens. In our study, it took less than two minutes for samples to reach the photostationary state under UV illumination. In Figure 7a, we can find that among four H-bonded CMS, the initial helical pitch length of BNAzo-MBA is the lowest, which is similar to that of BNAzo and

followed by BNAzo-DBA while those of BNAzo-(S)-OyBp and BNAzo-(R)-OyBp are highest, suggesting that HTP of BNAzo-MBA is the largest and those of BNAzo-(S)-OyBp and BNAzo-(R)-OyBp are the smallest. According to the equation we mentioned above, the corresponding change in HTP values were summarized in Table 1, when phototunability of H-bonded CMS in N-LCs host were measured. As shown in Table 1, the HTP value of BNAzo-MBA is highest while BNAzo-(S)-OyBp and BNAzo-(R)-OyBp have the lowest HTP values. It is noteworthy that the change of HTP value of BNAzo and BNAzo-MBA are also the biggest. In order to explain the effects of molecular structure on the HTP of H-bonded, the optimized structures predicted by Gaussian 03 calculations at the B3LYP/6-31G(d) level will be discussed. Figure 8 shows the optimized structures of the chiral switches before and after UV irradiation. The molecular structures can be observed more visually by the optimized geometries. From an overall perspective, BNAzo-MBA is much smaller in molecular size than BNAzo-DBA, BNAzo-(S)-OyBp and BNAzo-(R)-OyBp and we can also find that BNAzo-MBA possesses a rod shape, while BNAzo-DBA, BNAzo-(S)-OyBp and BNAzo-(R)-OyBp have a bent shape. Furthermore, we employ molecular aspect ratio based on the molecular simulations to verify the HTP difference of H-bonded CMS. As demonstrated that, the molecular aspect ratio, defined as the ratio of the molecular length (L) to the molecular diameter (D) is estimated from the model calculation and is one of the important parameters contributing to reveal the structures of the molecules.[10d, 10e] Investigation has been reported that a chiral dopant will have larger twisting power when it is similar in structure to the host LC molecules.[10f] The LC host we used here is SLC1717, a mixture of several rod-shaped compounds. Therefore, we can expect that chiral dopant with a larger aspect ratio will exhibit a larger twisting power, because a larger L/D means the molecule is more rod-like. As listed in Figure 8, the results reveal that the L/D of the H-bonded CMS molecules plays a relevant role in impacting the HTPs of them, which coincides with our previous study.[18] For example, BNAzo-MBA exhibits the highest initial HTP and it has the largest molecular aspect ratio among these H-bonded CMS. BNAzo-(S)-OyBp and BNAzo-(R)-OyBp have the lowest initial HTP values and the aspect ratio of them are also the lowest. Besides, the decrease of HTP of CMS after UV irradiation can also be explained by the optimized structures predicted by the B3LYP/6-31G(d) level and the molecular aspect ratio. Figure 8 shows that the aspect ratio decreased after UV irradiation, which means *cis* form has a greater bent degree than *trans* form and the HTP value became smaller during the photoisomerization accordingly. However, it is worth mentioning that the change of HTP we obtained through Cano-wedge method seems to be inconsistent with the aspect ratio based on the molecular simulation. We believe that it might be attributed to the difference between the molar mass of the four groups of CMS. For example, BNAzo-MBA has the lowest molar mass (908) while the molar mass of BNAzo-DBA is 1260. Since we used constant weight fraction in our study, it means that molar concentration is highest for the mixture with the H-bonded CMS of lowest molar mass. That might be the reason why the change of L/D of BNAzo-MBA is the lowest but the change of HTP of it is the highest. Moreover, although BNAzo-(S)-OyBp and BNAzo-(R)-OyBp have the same molecular characteristics except for opposite chirality, the HTP values measured did not differ significantly between them, which indicates that the tetrahedral chirality of two different donors is less efficient in comparison to much more efficient axial chirality of BNAzo.[13]

Table 1. Helical twisting power (in SLC1717) of H-bonded CMS and BNAzo at initial state (20 °C) and photostationary state (20 °C) upon UV irradiation (365nm, 2 mW·cm^{-2}) and at different temperatures (30 °C and 70 °C)

H-bonded Chiral Molecular Switches	HTP (wt%)/μm^{-1}		Ä HTP μm^{-1}[a]	* HTP[b] %	HTP (wt%)/μm^{-1}		Ä HTP (μm^{-1})[c]	* HTP[b] %
	Initial	PSS$_{UV}$			30°C	70°C		
BNAzo	52.7	41.5	11.2	21.3	46.0	40.5	5.5	11.9
BNAzo-MBA	53.9	40.1	13.8	25.6	49.4	35.1	14.3	34.7
BNAzo-DBA	36.2	31.5	4.7	13.0	35.0	26.1	8.9	25.3
BNAzo-(S)-OyBp	31.3	26.9	4.4	14.2	28.6	22.6	6.0	21.1
BNAzo-(R)-OyBp	32.0	27.3	4.7	14.6	28.7	23.0	5.7	20.0

[a] ΔHTP is calculated by subtracting the photostationary HTP value from the initial HTP value.

[b] * HTP means The change in HTP is calculated by dividing ΔHTP by initial HTP.

[c] ΔHTP is calculated by subtracting the 70°C HTP value from the 30°C HTP value.

The thermoresponsive behavior of Ch-LCs based on the H-bonded CMS was studied in the same way. Figure 7b shows the helical pitch length of BNAzo, BNAzo-MBA, BNAzo-DBA, BNAzo-(S)-OyBp and BNAzo-(R)-OyBp increase as the temperature increases, in other words, HTP values of these H-bonded CMS decrease with the temperature increasing. This result may have the following explanations. First, this is mainly because of the change in the orientation paramerter of the LC molecule induced by the weakened H-bonded interaction of H-bonded CMS.[22] Secondly, other factors, such as the perturbation of the bulk LCs (SLC-1717) at high temperatures and the change of binaphthyl twist angle induced by temperature (Table 1), may also contribute to the change of the HTP value. Meanwhile, we can also observe similar change in distance between Cano lines under various temperatures (Figure 7d). The length of helical pitch of BNAzo-(R)-OyBp was measured to be 3.48 μm at 30 °C and 4.35 μm at 70 °C, and for the BNAzo-(S)-OyBp, the pitch length increased from 3.49 μm (30 °C) to 4.43 μm (70 °C). According to the change of HTP values we summarized in Table 1, BNAzo-MBA has the most significant change in HTP value, it is possible that MBA has a more flexible ability to change the orientation of LC molecules in comparison to that of DBA, (R)-OyBp, and (S)-OyBp. Additionally, we could also find the change of HTP of BNAzo is 11.9%, which is smaller than changes of any other four Ch-LCs system based on H-bonded CMS (34.7%, 25.3%,

21.1%, 20.0%), so we can conclude that H-bonds between the carboxylic acid and pyridyl group contribute to the temperature dependence of HTP in the H-bonded CMS.

As mentioned above, Ch-LCs can selectively reflect light, so we studied the temperature and irradiation time dependence of the selective reflection bands (SRB) of H-bonded CMS with N-LCs host. We prepared mixtures and the corresponding weight ratios are BNAzo-MBA: SLC1717 = 5:95 and other three chiral dopants (BNAzo-DBA, BNAzo-(S)-OyBp and BNAzo-(R)-OyBp) : SLC1717 = 10:90. Then we put the samples into glass cells. The glass cells were composed of two glass substrates, which were coated with a 3.0 wt% polyvinyl alcohol aqueous solution and subsequently rubbed with a textile cloth in one direction to generate a planar alignment. Figure 9 shows the irradiation time and temperature dependence of the reflection bands of BNAzo-MBA, BNAzo-DBA, BNAzo-(S)-OyBp and BNAzo-(R)-OyBp respectively. As shown in Figure 9a，the reflection bands of all the samples increased with the increasing irradiation time of UV light (365nm, 6 $mW \cdot cm^{-2}$) coinciding with the changes of HTP shown in Table 1. For example, the reflection wavelength of BNAzo-DBA experiences a red shift from 542 nm (0s) to 713 nm (120s) due to photoisomerization. Meanwhile, with the increasing temperature, the reflection wavelength of all the samples undergoes a red shift, which is also corresponding to the results we discussed above. As is shown in Figure 9b，reflection wavelength of BNAzo-(S)-OyBp increases from 597 nm (30 °C) to 759 nm (70°C) attributed to the modulation of the intermolecular forces between the proton donors and acceptors as temperature increases.

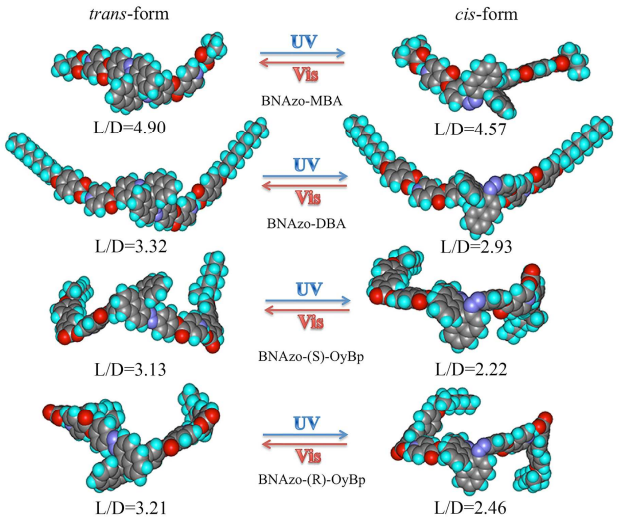

Figure 8. Optimized structures of *trans* and *cis* form of BNAzo-MBA, BNAzo-DBA, BNAzo-(S)-OyBp, BNAzo-(R)-OyBp (space filling model) obtained by Gaussian 03 calculations at the B3LYP/6-31G(d) level.

Given the high HTPs as well as the remarkable variation in HTP values upon UV light irradiation and heat treatment, we filled a mixture of 8.1 wt% BNAzo-MBA in SLC1717 into a 10 μm thick planar aligned cell to observe the change of SRB of the Ch-LCs. The reflection central wavelength was around 490 nm at the initial state. Upon UV irradiation, its reflection wavelength was tuned to 550 nm in only 30s and reached a photostationary state in 60 s with a reflection central wavelength at around 700 nm (Figure 10a). It is noteworthy that the process is reversible by visible light irradiation (450 nm,

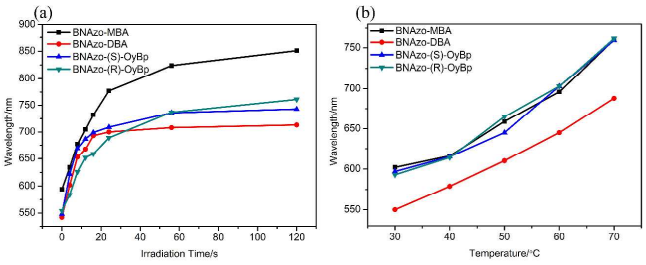

Figure 9. (a) The irradiation time dependence of SRB of H-bonded CMS in SLC1717 in a 10 μm thick planar cell under UV light irradiation (365nm, 6 $mW \cdot cm^{-2}$) for 0s, 4s, 8s, 12s, 16s, 24s, 56s and 120s and (b) The temperature dependence of SRB of H-bonded CMS in SLC1717 at various temperatures (from 30°C to 70°C).

15mW/cm^2) for 60 s or keeping it in the dark room at 50 °C for 2h. Likewise, we can find that the reflection wavelength was tuned from 490 nm to 640 nm as the temperature increased from 25 °C to 65 °C and it is also thermally reversible. (Figure 10b) Furthermore, four reflection colors (red, green, yellow and blue) can be observed in both glass cells filled with the same LCs sample, suggesting that we have successfully fabricated LCs sensors that change reflection color upon exposure to UV light as well as heat treatment by doping H-bonded CMS into achiral N-LCs host.

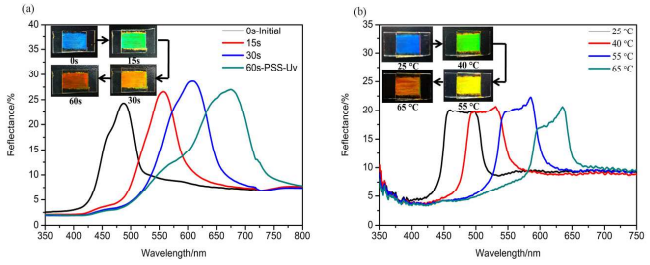

Figure 10. Reflection spectra of 8.1 wt% BNAzo-MBA in SLC1717 in 10 μm thick planar cells under UV irradiation (a) and at various temperatures (b). The insets are photographs of the cells.

Conclusions

In summary, we fabricated four H-bonded chiral molecular switches (BNAzo-MBA, BNAzo-DBA, BNAzo-(S)-OyBp and BNAzo-(R)-OyBp), and photo/thermo reversible tuning behavior of cholesteric liquid crystals based on the H-bonded chiral molecular switches were investigated. The reflection bands of all the cholesteric liquid crystals mixtures exhibited red shift under UV irradiation as well as with an increase of temperature. The isomerization of azobenzene moieties in H-bonded chiral molecular switches under UV/visible light is

responsible for good phototunability. Meanwhile, the modulation of interaction between H-bonded donors and acceptors with temperature plays one of the important roles for the temperature-sensitivity of the Ch-LCs. What's more, the optimized molecular structures obtained by Gaussian 03 calculations at the B3LYP/6-31G(d) level suggest that the introduction of rigid units such as phenyl or biphenyl group in BNAzo-DBA, BNAzo-(S)-OyBp and BNAzo-(R)-OyBp can bend the molecular switches and lead to a difference in HTP value of the four groups of the switches. Additionally, the HTP values of BNAzo-(S)-OyBp and BNAzo-(R)-OyBp are similar despite of opposite handedness of their proton donors, which is probably due to the less efficient tetrahedral chirality of two different donors in comparison to much more efficient axial chirality of BNAzo in our H-bonded self-assembled system.

Acknowledgements

This research was supported by the National Natural Science foundation (Grant no. 51373013, 51173013 and 50903004) and Beijing Young Talents Plan (YETP0489). We also thank CHEMCLOUDCOMPUTING of Beijing University of Chemical Technology for the molecular simulation of this investigation.

College of Materials Science and Engineering, Beijing University of Chemical Technology, Beijing 100029, P. R. China.
E-mail: guojb@mail.buct.edu.cn

Notes and references

1 (a) S. Pieraccini, S. Masiero, A. Ferrarini and S. G. Piero, *Chem. Soc. Rev.*, 2011, **40**, 258-271; (b)E. Sackmann, *J. Amer. Chem. Soc.*, 1971, **93**, 7088-7090; (c) A. Ryabchun, A. Bobrovsky, A. Sobolewska, V. Shibaev and J. Stumpe, *J. Mater. Chem.*, 2012, **22**, 6245-6250.

2 (a) Q. Li, Y. Li, J. Ma, D.-K. Yang, T. J. White and T. J. Bunning, *Adv. Mater. (Weinheim, Ger.)*, 2011, **23**, 5069-5073; (b)Y. Li, A. Urbas and Q. Li, *J. Am. Chem. Soc.*, 2012, **134**, 9573-9576; (c) M. Mitov, *Adv. Mater.*, 2012, **24**, 6260-6276.

3 K. S. Burnham and G. B. Schuster, *J. Am. Chem. Soc.*, 1998, **120**, 12619-12625.

4 M. Mathews, R. S. Zola, D.-k. Yang and Q. Li, *J. Mater. Chem.*, 2011, **21**, 2098-2103.

5 (a) C. Ruslim and K. Ichimura, *J. Mater. Chem.*, 2002, **12**, 3377-3379; (b) C. Xue, K. Gutierrez-Cuevas, M. Gao, A. Urbas and Q. Li, *J. Phys. Chem. C*, 2013.

6 S. A. Holmstrom, L. V. Natarajan, V. P. Tondiglia, R. L. Sutherland and T. J. Bunning, *Appl. Phys. Lett.*, 2004, **85**, 1949-1951.

7 (a) A. Bobrovsky, N. Boiko and V. Shibaev, *Macromolecules*, 2006, **39**, 6367-6370; (b) M. Teng, D. Wang, X. Jia, X. Fan, G. Kuang, X. Chen, D. Zou and Y. Wei, *J. Phys. Chem. C*, 2011, **115**, 22540-22546; (c) M. Mathews and N. Tamaoki, *J. Am. Chem. Soc.*, 2008, **130**, 11409-11416; (d) H. Akiyama, A. Tanaka, H. Hiramatsu, J. i. Nagasawa and N. Tamaoki, *J. Mater. Chem.*, 2009, **19**, 5956.

8 (a) Y. Wang, A. Urbas and Q. Li, *J. Am. Chem. Soc.*, 2012, **134**, 3342-3345; (b) B. L. Feringa, *J. Org. Chem.*, 2007, **72**, 6635-6652.

9 (a) K. Rameshbabu, A. Urbas and Q. Li, *J. Phys. Chem. B*, 2011, **115**, 3409-3415; (b) T. van Leeuwen, T. C. Pijper, J. Areephong, B. L. Feringa, W. R. Browne and N. Katsonis, *J. Mater. Chem.*, 2011, **21**, 3142-3146; (c) H. Hayasaka, T. Miyashita, M. Nakayama, K. Kuwada and K. Akagi, *J. Am. Chem. Soc.*, 2012, **134**, 3758-3765; (d) S. Pieraccini, G. Gottarelli, R. Labruto, S. Masiero, O. Pandoli and G. P. Spada, *Chem. - Eur. J.*, 2004, **10**, 5632-5639; (e) Y. Li, M. Wang, T. J. White, T. J. Bunning and Q. Li, *Angew. Chem. Int. Ed.*, 2013, **52**, 8925-8929; (f) L. Green, Y. Li, T. White, A. Urbas, T. Bunning and Q. Li, *Org. Biomol. Chem.*, 2009, **7**, 3930-3933; (g) B. S. Udayakumar and G. B. Schuster, *J. Org. Chem.*, 1993, **58**, 4165-4169; (h) L.-M. Jin, Y. Li, J. Ma and Q. Li, *Org. Lett.*, 2010, **12**, 3552-3555; (i) S. Pieraccini, S. Masiero, G. P. Spada and G. Gottarelli, *Chem. Commun.*, 2003, **5**, 598-599.

10 (a) Y. Yu, M. Nakano and T. Ikeda, *Nature*, 2003, **425**, 145; (b) K. Ichimura, S.-K. Oh and M. Nakagawa, *Science (Washington, D. C.)*, 2000, **288**, 1624-1626; (c) S. Kurihara, T. Yoshioka, T. Ogata, Z. A. Md and T. Nonaka, *Liq. Cryst.*, 2003, **30**, 1219-1223; (d) T. Yoshioka, T. Ogata, *Adv. Mater.(Weinheim, Ger.)*, 2005, **17**, 1226-1229; (e) M. Z. Alam, T. Yoshioka, T. Ogata, T. Nonaka, S. Kurihara, *Liq. Cryst.*, 2007, **34**, 1215-1219; (f) C. Ruslim and K. Ichimura, *Adv. Mater. (Weinheim, Ger.)*, 2001, **13**, 37-40.

11 M. Irie, *Chem. Rev. (Washington, D. C.)*, 2000, **100**, 1685-1716.

12 Y. Li, A. Urbas and Q. Li, *J. Org. Chem.*, 2011, **76**, 7148-7156.

13 (a) M. Mathews, R. S. Zola, S. Hurley, D.-K. Yang, T. J. White, T. J. Bunning and Q. Li, *J. Am. Chem. Soc.*, 2010, **132**, 18361-18366; (b) T. J. White, R. L. Bricker, L. V. Natarajan, N. V. Tabiryan, L. Green, Q. Li and T. J. Bunning, *Adv. Funct. Mater.*, 2009, **19**, 3484-3488; (c) J. Ma, Y. Li, T. White, A. Urbas and Q. Li, *Chem. Commun.*, 2010, **46**, 3463-3465; (d) Y. Li and Q. Li, *Org. Lett.*, 2012, **14**, 4362-4365; (e) Y. Wang and Q. Li, *Adv. Mater.*, 2012, **24**, 1926-1945.

14 (a) A. Demenev, S. H. Eichhorn, T. Taerum, D. F. Perepichka, S. Patwardhan, F. C. Grozema, L. D. A. Siebbeles and R. Klenkler, *Chem. Mater.*, 2010, **22**, 1420-1428; (b) P. V. Shibaev, J. Madsen and A. Z. Genack, *Chem. Mater.*, 2004, **16**, 1397-1399; (c) G. A. Shandryuk, S. A. Kuptsov, A. M. Shatalova, N. A. Plate and R. V. Talroze, *Macromolecules*, 2003, **36**, 3417-3423; (d) H. Kihara, T. Kato, T. Uryu and J. M. J. Fréchet, *Chem. Mater.*, 1996, **8**, 961-968; (e) T. J. White, M. E. McConney and T. J. Bunning, *J. Mater. Chem.*, 2010, **20**, 9832-9847; (f) C. Ohm, M. Brehmer and R. Zentel, *Adv. Mater.*, 2010, **22**, 3366-3387; (g) H. Yu and T. Ikeda, *Adv. Mater.*, 2011, **23**, 2149-2180; (h) D. J. Broer, C. M. W. Bastiaansen, M. G. Debije and A. P. H. J. Schenning, *Angew. Chem. Int.Ed.*, 2012, **51**, 7102-7109; (i) D. J. Mulder, A. P. H. J. Schenning and C. W. M. Bastiaansen, *J. Mater. Chem. C.*, 2014, **2**, 6695-6705.

15 (a) F. J. Chen, J. B. Guo, Z. J. Qu and J. Wei, *J. Mater. Chem.*, 2011, **21**, 8574-8582; (b) F. J. Chen, J. B. Guo, O. Y. Jin and J. Wei, *Chin. J. Polym. Sci.*, 2013, **31**, 630-640.

16 (a) T. Kato and J. M. J. Frechet, *J. Am. Chem. Soc.*, 1989, **111**, 8533-8534; (b) T. Kato, M. Fukumasa and J. M. J. Frechet, *Chem. Mater.*, 1995, **7**, 368-372.

17 N. Herzer, H. Guneysu, D. J. D. Davies, D. Yildirim, A. R. Vaccaro, D. J. Broer, C. W. M. Bastiaansen and A. P. H. J. Schenning, *J. Am. Chem. Soc.*, 2012, **134**, 7608-7611.

18 Y. Xie, D. Fu, O. Jin, H. Zhang, J. Wei and J. Guo, *J. Mater. Chem. C.*, 2013, **1**, 7346-7356.

19 T. Kato, J. M. Frechet, P. G. Wilson, T. Saito, T. Uryu, A. Fujishima, C. Jin and F. Kaneuchi, *Chem. Mater.*, 1993, **5**, 1094-1100.
20 H. Goto and K. Kawabata, *Polym. Chem.*, 2011, **2**, 1098-1106.
21 T. Ikeda, *J. Mater. Chem.*, 2003, **13**, 2037-2057.
22 A. Takahashi, V. A. Mallia and N. Tamaoki, *J. Mater. Chem.*, 2003, **13**, 1582-1587.